

# The E288K Colon Tumor Variant of DNA Polymerase $\beta$ Is a Sequence Specific Mutator

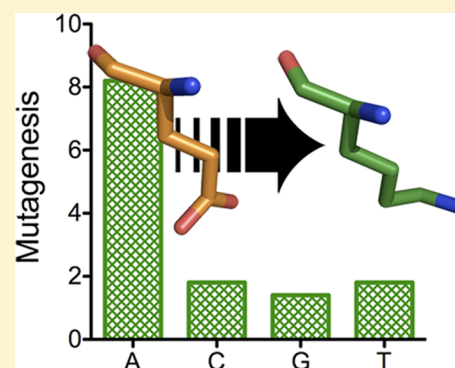
Drew L. Murphy,<sup>†</sup> Katherine A. Donigan,<sup>‡</sup> Joachim Jaeger,<sup>§</sup> and Joann B. Sweasy<sup>\*,†,‡</sup>

<sup>†</sup>Department of Therapeutic Radiology and <sup>‡</sup>Department of Genetics, Yale University School of Medicine, New Haven, Connecticut 06520, United States

<sup>§</sup>Wadsworth Center, New York State Department of Health, Center for Medical Science, 150 New Scotland Avenue, Albany, New York 12208, United States

## S Supporting Information

**ABSTRACT:** DNA polymerase  $\beta$  (pol  $\beta$ ) is the main polymerase involved in base excision repair (BER), which is a pathway responsible for the repair of tens of thousands of DNA lesions per cell per day. Our recent efforts in sequencing colon tumors showed that 40% of the tumors sequenced possessed a variant in the coding region of the *POLB* gene; one of these variants is E288K. Expression of the E288K variant in cells leads to an increase in the frequency of mutations at AT base pairs. In vitro, the E288K variant is as active as and binds one-base-gapped DNA with the same affinity as wild-type pol  $\beta$ . Single-turnover kinetic data for the E288K variant show that its mutator phenotype is specific for misincorporating opposite template A up to 6-fold more than the wild-type enzyme and that this is due to a decrease in the degree of discrimination in nucleotide binding. Molecular modeling suggests that the substitution of Lys at position 288 causes the polymerase to adopt a more open conformation, which may be disrupting the nucleotide binding pocket. This may explain the reduced degree of discrimination at the level of nucleotide binding. The enhanced mutagenesis of the E288K variant could lead to genomic instability and ultimately a malignant tumor phenotype.



Base excision repair (BER) is responsible for the repair of tens of thousands of endogenous DNA lesions per cell per day.<sup>1</sup> In BER, the damage is recognized and removed by DNA glycosylases that have overlapping specificity for small base damage. In the case of monofunctional glycosylases, APE1 then cleaves the DNA backbone, which leaves behind a one-base-gapped DNA with a 5'-deoxyribose phosphate (dRP) moiety.<sup>2</sup> DNA polymerase  $\beta$  (pol  $\beta$ ) fills in the resulting gap in the DNA and removes the dRP group. In the case of bifunctional glycosylases, the base is removed and the DNA is cleaved. After the ends have been remodeled to generate a 3'-hydroxyl and 5'-phosphate, pol  $\beta$  fills in the gap. Once the gap has been filled, the complex of XRCC1 and LigIII $\alpha$  seals the backbone to complete the repair. The correct repair of these lesions is critical for genomic integrity.

Pol  $\beta$  is the main polymerase involved in BER, and as such, it has control over the fidelity of the DNA synthesis at the one-base gap. Pol  $\beta$  is a small (39 kDa), error-prone polymerase that does not possess any inherent proofreading capability, inserting an incorrect nucleotide in one of every 10000 nucleotides.<sup>3</sup> Any errors introduced into the DNA by pol  $\beta$  can lead to a mutator phenotype. A mutator phenotype is associated with cancer.<sup>4</sup> Additionally, variants of pol  $\beta$  have been found in wide variety of cancerous tissues.<sup>3</sup> Many of these cancer-associated variants have been shown to have aberrant function(s).<sup>5–9</sup> In our recent sequencing of colon tumors

(unpublished results of K. A. Donigan), coding region variants of pol  $\beta$  were found in 40% of the 134 tumors sequenced. Preliminary data suggested that one of the variants found in these tumors, E288K, might be a mutator polymerase.

In this study, the E288K variant of pol  $\beta$  was determined to be a mutator in vivo. In a forward mutation assay in mammalian cells, expression of E288K increased the frequency of mutations at AT base pairs by 3-fold versus that in cells not expressing E288K. This mutator phenotype was also observed in vitro, where under single-turnover conditions the E288K variant showed decreased fidelity on one-base-gapped DNA with a template A compared to the wild-type polymerase. Additionally, this loss of fidelity was specific for adenine templates, as results with DNA substrates with other template bases were the same as those with wild-type pol  $\beta$ .

## EXPERIMENTAL PROCEDURES

**Mutant Construction and Protein Expression and Purification.** Wild-type pol  $\beta$  with an N-terminal six-His tag was previously cloned into the pET28a expression vector.<sup>10</sup> The G to A mutation at codon 288 (encoding the E288K variant) was introduced into the wild-type plasmid using the

Received: March 19, 2012

Revised: May 29, 2012

Published: May 31, 2012



**Table 1. One-Base-Gapped DNA Substrates Used in This Study, Constructed from Oligonucleotides Listed in Table S2 of the Supporting Information**

DNA Substrate	Sequence	Oligos Used
KDA	5' - GGATTTGTTTCAGAACGCTCGGT GCCGCCGGGCGTTTGTATTGG 3' - CCTAAACAAGTCTTGCAGGCCA <u>A</u> CGGCGGCCCGCAAACAATAACC	AP+AD+AT
C2R	5' - TCTTGAATGGTGGGTCGTTGAC ACGACATGGCTCGATTGGCGCG 3' - AGAACTTACCACCCAGCAACTG <u>C</u> TGCTGTACCGAGCTAACCGCGC	CP+CD+CT
C2	5' - CGCGCCAATCGAGCCATGTCGT GTCAACGACCCACCATTCAAGA 3' - GCGCGGTTAGCTCGGTACAGCA <u>G</u> CAGTTGCTGGGTGGTAAGTTCT	GP+GD+GT
KDAR	5' - CCAATAACAAACGCCCGCGGC TCCGAGCGTTCTGAACAAATCC 3' - GGTTATTGTTTGCGGGCGCGC <u>T</u> AGGCTCGCAAGACTTGTTTAGG	TP+TD+TT

QuikChange site-directed mutagenesis kit (Stratagene) and specific polymerase chain reaction (PCR) primers (Table S1 of the Supporting Information). Both wild-type and E288K pol  $\beta$  were expressed in *Escherichia coli* BL21(DE3) and purified via fast protein liquid chromatography as previously described.<sup>11</sup>

**DNA Substrates for Kinetic Assays.** One-base-gapped DNA substrates with A and G templating bases were based on the *lacII* gene. The substrates with T and C templating bases are the reverse complements of the A and G substrates, respectively. DNA oligonucleotides were ordered from the Keck Oligo Synthesis Resource at the Yale School of Medicine and purified by polyacrylamide gel electrophoresis. DNA substrates containing a one-base gap were constructed by annealing two 22-mers (5'-<sup>32</sup>P-labeled primer and 5'-PO<sub>4</sub>-downstream oligo) to a complementary 45-mer template oligo, as previously described.<sup>10</sup> The oligos listed in Table S2 of the Supporting Information were used to construct all the DNA substrates used in this study (see Table 1).

**Circular Dichroism Spectroscopy.** Circular dichroism spectra were recorded for the wild type and E288K using a Chirascan circular dichroism spectrometer (Applied Photophysics). The ellipticity of a 1  $\mu$ M solution of pol  $\beta$  in 10 mM K<sub>2</sub>HPO<sub>4</sub> at 23 °C was measured from 280 to 190 nm with a path length of 2 mm. The same sample was then used to measure the thermal denaturation profile of the pol  $\beta$  proteins. Starting at 5 °C, the temperature was slowly increased to 65 °C at a rate of 1 °C/min while the ellipticity at 222 nm was measured.

**Pre-Steady-State Burst Assay.** Rapid chemical quench kinetics were performed using the KinTek Chemical Quench-Flow (RQF-3) apparatus.<sup>12</sup> Experiments were conducted using one-base-gapped DNA [KDA, template A (Table 1)] and the correct nucleotide (dTTP) as previously described.<sup>11</sup> Kinetic data were plotted and fit using Prism 5 (GraphPad Software, Inc.) to the biphasic burst equation:

$$[\text{product}] = [E]_{\text{app}} \left\{ \frac{k_{\text{obs}}^2}{k_{\text{obs}} + k_{\text{ss}}} [1 - e^{-(k_{\text{obs}} + k_{\text{ss}})t}] + \frac{k_{\text{obs}}k_{\text{ss}}}{k_{\text{obs}} + k_{\text{ss}}} t \right\}$$

where  $[E]_{\text{app}}$  is the apparent enzyme concentration,  $k_{\text{obs}}$  is the observed rate constant of the exponential phase, and  $k_{\text{ss}}$  is the rate constant of the linear (steady-state) phase.

**Active Site Titration.** Under the same conditions that were used for the pre-steady-state burst described above, one-base-gapped DNA [KDA, template A (Table 1)] was titrated into the polymerase reaction mixture. Reactions were conducted in the KinTek apparatus as described above for 0.15 s. This time point was chosen on the basis of the pre-steady-state burst data (Figure 1) to yield maximal product formation with a minimal contribution from multiple enzyme turnovers. A total of four reactions were conducted for each DNA concentration (from 10 to 300 nM, final concentration). Reactions were analyzed as described above; the average amount of product formed was plotted versus DNA concentration, and the data were fit using Prism 5 (GraphPad Software, Inc.) to the following quadratic active site titration equation:

$$[\text{product}] = 0.5[K_{\text{D(DNA)}} + \text{AS} + [\text{DNA}]] - \{0.25[K_{\text{D(DNA)}} + \text{AS} + [\text{DNA}]]^2 - \text{AS} \times [\text{DNA}]\}^{0.5}$$

where  $K_{\text{D(DNA)}}$  is the equilibrium dissociation constant for DNA, AS is the percent active sites of the protein preparation, and [DNA] is the concentration of DNA in nanomolar.

**Cell Lines.** GP2-293 cells (Clontech) were used for viral packaging and maintained in DME10 [Dulbecco's modified Eagle's medium (Gibco) supplemented with 10% fetal bovine serum (FBS; Gemini Bio-Products) and 1% penicillin-streptomycin (Gibco)] with 1% L-glutamine and 1 mM HEPES (Gibco). C127 $\lambda$ b, murine mammary carcinoma cells from an RIII mouse (ATCC) that have multiple copies of  $\lambda$  phage DNA integrated into the genome, were grown in DME10 with 0.6 mg/mL G418 (Gibco) added to maintain the  $\lambda$  DNA integration. All cell lines were grown at 37 °C in a humidified 5% CO<sub>2</sub> incubator.

**Transfection, Infection, and Expression Analysis.** Retrovirus production was conducted by cotransfecting GP2-293 cells with a pRVYtet-pol  $\beta$  plasmid and pVSVG as previously described.<sup>8</sup> Single clones of C127 $\lambda$ b cells were prepared by retroviral infection and selection as previously described<sup>8</sup> with modified selection criteria (160  $\mu$ g/mL hyg and 0.6 mg/mL G418). Exogenous pol  $\beta$  expression in clones

generated in this system can be induced in a “tet-off” manner; expression is turned off in the presence of 4  $\mu\text{g/mL}$  tetracycline (Sigma) and turned on in the absence of tetracycline. Expression of pol  $\beta$  in C127 $\lambda$ b cells was monitored by Western blotting as previously described.<sup>8</sup> Only C127 $\lambda$ b clones that had approximately equal levels of expression of exogenous and endogenous pol  $\beta$  and no exogenous expression in the presence of 4  $\mu\text{g/mL}$  tet were selected for use in experiments.

**Preparation of High-Molecular Weight DNA for the  $\lambda$ cII Forward Mutation Assay.** A pair of 75  $\text{cm}^2$  flasks of a C127 $\lambda$ b clone were seeded and the contents allowed to grow to confluence, one in 4  $\mu\text{g/mL}$  tet (not expressing E288K pol  $\beta$ ) and one in the absence of tet (expressing E288K pol  $\beta$ ). Attached cells were washed twice with 1 $\times$  PBS (Gibco) and incubated for 5 min at room temperature in extraction buffer [10 mM Tris (pH 8), 0.1 M EDTA, and 0.5% SDS]. The resulting cell slurry was transferred to a 15 mL tube; RNaseA was added to a final concentration of 20  $\mu\text{g/mL}$ , and the mixture was incubated at 37  $^\circ\text{C}$  for 1 h. Proteinase K was added to a final concentration of 100  $\mu\text{g/mL}$ , and the mixture was incubated at 37  $^\circ\text{C}$  overnight. The resulting extract was cooled to room temperature and extracted once with a phenol/chloroform/isoamyl alcohol mixture and once with chloroform. The aqueous DNA solution was then dialyzed against TE buffer four times at 4  $^\circ\text{C}$ . A  $1/10$  volume of 3 M sodium acetate (pH 3.2) was added to the DNA solution, and 2 volumes of ice-cold 200 proof ethanol was added to precipitate the genomic DNA. The DNA was removed from the liquid using a glass hook, air-dried in a microcentrifuge tube, and dissolved in TE.

**$\lambda$ cII Forward Mutation Assay.** Sonication and freeze-thaw packaging extracts were prepared as previously described.<sup>13,14</sup> To package the DNA into phage, approximately 5  $\mu\text{g}$  of the genomic DNA from the C127 $\lambda$ b cells was added to 95  $\mu\text{L}$  of packaging extracts and incubated at 32  $^\circ\text{C}$  for 90 min. An additional 95  $\mu\text{L}$  of packaging extracts was added and incubated at 32  $^\circ\text{C}$  for an additional 90 min. Packaged phage were then diluted in phage lambda buffer [6 mM Tris (pH 7.2), 10 mM  $\text{MgSO}_4$ , and 0.005% gelatin], mixed with G1250 *E. coli*, and incubated at room temperature for 40 min. The G1250/phage mixture was then mixed with 3 mL of 0.4% top agar and poured onto TB plates. Plates were incubated at 37  $^\circ\text{C}$  to determine the infection titer, and other plates were incubated at 24  $^\circ\text{C}$  to determine the number of plaques from phage harboring a mutation in the  $\lambda$ cII gene. The mutation frequency was calculated as the ratio of the number of mutant plaques to the total number of plaques plated. At least 770000 total plaques were plated over at least three different packaging reactions for each DNA (from cells either expressing or not expressing E288K pol  $\beta$ ). Average mutation frequencies are reported for each treatment.

**$\lambda$ cII Mutation Analysis.** Mutant plaques were purified by replating on G1250 as described above. Phage DNA was isolated by suspending top agar plugs of plaques in 0.1% Tween 20. The  $\lambda$ cII gene was amplified from the phage DNA using the cII primers (Table S1 of the Supporting Information). The PCR mixture [1  $\mu\text{L}$  of phage DNA, primers (0.5  $\mu\text{M}$  each), 0.2 mM dNTPs, 3.7 mM  $\text{MgCl}_2$ , 0.75 unit of Taq (Invitrogen), and 1 $\times$  Taq buffer (Invitrogen), in a total volume of 25  $\mu\text{L}$ ] was denatured at 95  $^\circ\text{C}$  for 1 min and cycled (95  $^\circ\text{C}$  for 30 s, 53  $^\circ\text{C}$  for 40 s, and 72  $^\circ\text{C}$  for 1 min) 35 times. The PCR products were purified using shrimp alkaline phosphatase (USB) and exonuclease I (NEB) and sequenced using the “cII F” PCR

primer at the Keck DNA Sequencing Lab at the Yale University School of Medicine.

**Single-Turnover Kinetics.** The kinetics of incorporation of the correct nucleotide on all DNA substrates listed in Table 1 was measured using the KinTek apparatus as previously described.<sup>11</sup> Briefly, 500 nM active pol  $\beta$  (determined by active site titration, described above) and 50 nM one-base-gapped DNA were reacted with varying concentrations of correct nucleotide (0.5 to 450  $\mu\text{M}$ ) for various times (0.01 to 10 s). Incorrect nucleotide incorporations were conducted manually under the same reaction conditions that were used for correct nucleotide incorporation. Nucleotide concentrations ranged from 0.1 to 1500  $\mu\text{M}$ , and reaction times varied from 10 s to 60 min. For both correct and incorrect incorporations, reactions were quenched with EDTA and products were separated on polyacrylamide sequencing gels. The gels were analyzed using a Storm 860 phosphorimager with ImageQuant. Kinetic data were plotted and fit using Prism 5 (GraphPad Software, Inc.) to the following single-exponential equation:

$$[\text{product}] = A(1 - e^{-k_{\text{obs}}t})$$

where  $k_{\text{obs}}$  is the observed rate constant for a particular dNTP concentration. Each of the observed rate constants was then plotted versus dNTP concentration and fit to the hyperbolic equation

$$k_{\text{obs}} = \frac{k_{\text{pol}}[\text{dNTP}]}{K_{\text{d(dNTP)}} + [\text{dNTP}]}$$

where  $k_{\text{pol}}$  is the maximal rate of polymerization and  $K_{\text{d(dNTP)}}$  is the equilibrium dissociation constant for dNTP.

**Molecular Modeling.** Molecular modeling for pol  $\beta$  E288K with either dTTP or dCTP in the active site opposite template A was performed as previously described.<sup>11</sup>

## RESULTS

**Pol  $\beta$  E288K Possesses Overall Properties Similar to Those of the Wild-Type Polymerase.** The circular dichroism spectra and thermal denaturation curves (Figure S1 of the Supporting Information) for E288K and wild-type pol  $\beta$  are indistinguishable from one another. This indicates that both polymerases have the same secondary structure content and thermal stability; however, this does not rule out small, subtle differences in the local structure of the polymerase. Additionally, the E288K variant polymerase possesses the same pre-steady-state kinetic burst profile (Figure 1) as the wild-type pol  $\beta$ , suggesting that both E288K and wild-type pol  $\beta$  employ the same overall kinetic mechanism. Here, a rapid, first-order chemistry step is followed by a slower, product release step. Both the rate of polymerization ( $k_{\text{obs}}$ ) and rate of product release ( $k_{\text{ss}}$ ) are similar to that of the wild-type polymerase and previously reported pol  $\beta$  rates ( $k_{\text{obs}} = 8 \pm 1$  and  $13.8 \pm 0.5 \text{ s}^{-1}$  and  $k_{\text{ss}} = 0.6 \pm 0.2$  and  $0.68 \pm 0.06 \text{ s}^{-1}$  for the wild type and E288K, respectively).<sup>10,11,15</sup> To determine the equilibrium dissociation constant for DNA [ $K_{\text{D(DNA)}}$ ] and the percent of active sites in the protein preparation, we conducted active site titration for both the wild type and E288K (Figure 2). The E288K variant binds to one-base-gapped DNA with the same affinity as the wild-type polymerase [ $K_{\text{D(DNA)}} = 19 \pm 1$  and  $19 \pm 3 \text{ nM}$  for the wild type and E288K, respectively].

**The Pol  $\beta$  E288K Variant Has an Increased Mutation Frequency at AT Base Pairs.** To determine whether the E288K variant is a mutator in cells, the  $\lambda$ cII forward mutation



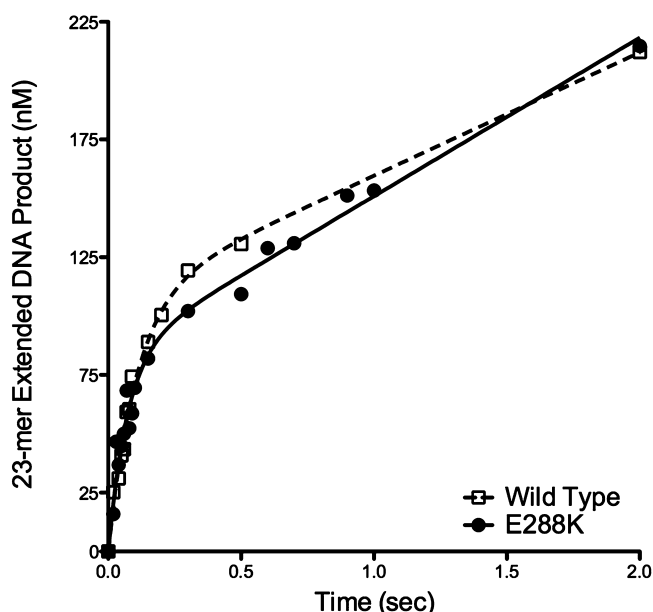


**Figure 1.** Representative pre-steady-state plots of extended DNA product vs time for the wild type and E288K. Both E288K and the wild type exhibit biphasic kinetics, which indicates that they are following the same overall mechanism [ $k_{\text{obs}} = 8 \pm 1$  and  $13.8 \pm 0.5 \text{ s}^{-1}$  and  $k_{\text{ss}} = 0.6 \pm 0.2$  and  $0.68 \pm 0.06 \text{ s}^{-1}$  for the wild type and E288K, respectively (averages  $\pm$  the standard error of the mean for three independent experiments)].

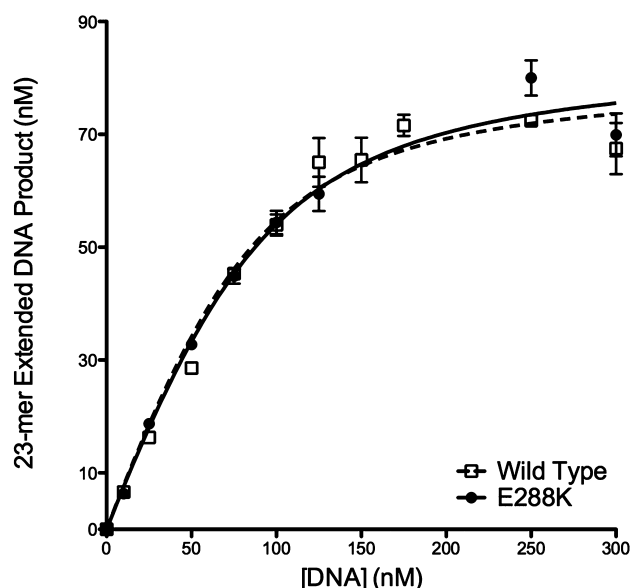


**Figure 2.** Representative active site titration plots of the extended DNA product vs DNA substrate concentration for the wild type and E288K. E288K and wild-type pol  $\beta$  both bind DNA with the same affinity [ $K_{\text{D(DNA)}} = 19 \pm 1$  and  $19 \pm 3 \text{ nM}$  for the wild type and E288K, respectively (average  $\pm$  the standard error of the mean for three independent experiments)].

assay was performed. A clonal cell line containing the  $\lambda$  phage genome (C127 $\lambda$ b) was generated expressing the E288K variant pol  $\beta$  in a “Tet Off” manner (Figure S2 of the Supporting Information) and was used to perform the forward mutation assay. Exogenous expression of the E288K variant had a weak effect on the overall mutation frequency seen in this assay [ $(2.5 \pm 0.5) \times 10^{-4}$  and  $(1.6 \pm 0.4) \times 10^{-4}$  for NoTet ( $n = 5$ ) and

Tet ( $n = 3$ ), respectively]. To determine the number and types of mutations generated by expressing E288K in C127 $\lambda$ b cells, the sequences of the *cII* mutants were analyzed. All of the mutations in the *cII* gene were plotted along the wild-type *cII* sequence to generate a mutation spectrum (Figure S3 of the Supporting Information), and it was determined that there was no hotspot in the *cII* gene that was especially susceptible to mutation by the E288K variant. However, tabulating the bases that were mutated in the *cII* gene revealed that E288K was 3-fold more likely than WT to generate mutations at AT base pairs in this sequence (Table 2). Because information about the

**Table 2. Specific Mutation Frequencies at Each of the Four DNA Bases from the  $\lambda$ cII Forward Mutation Assay<sup>a</sup>**

DNA base	no. of mutations		frequency ( $\times 10^{-5}$ )		NoTet/Tet
	NoTet	Tet	NoTet	Tet	
A or T	13	5	3.1	1.0	3.1
G or C	37	29	8.8	5.9	1.5
A	7	1	1.7	0.20	8
C	9	6	2.1	1.5	2
G	28	23	6.7	4.7	1
T	6	4	1.4	0.81	2

<sup>a</sup>The frequency was calculated as the number of mutants at a particular base divided by the total number of mutants multiplied by the average mutation frequency of that treatment (Tet or NoTet).

strandedness is not available in this assay, these could be mutations at either A or T, or a combination of both. The frequency of mutations at GC base pairs in the *cII* gene was increased 1.5-fold by expression of the E288K variant.

**The Pol  $\beta$  E288K Variant Misincorporates in Vitro opposite Template A.** To further examine the specific kinetic details of the E288K-induced mutagenesis, single-turnover kinetics assays were performed. By conducting assays under single-turnover conditions, we could determine both the maximal rate of polymerization ( $k_{\text{pol}}$ ) and equilibrium dissociation constant for dNTP [ $K_{\text{d(dNTP)}}$ ] for each nucleotide/template pair. Both the wild type and the E288K variant exhibit fast incorporation of the correct nucleotide opposite template A and a drastic decrease in the rate of polymerization for the incorrect nucleotide (Table 3), up to 1200-fold slower for incorrect incorporation. However, there is little difference in discrimination of correct from incorrect dNTPs at the level of  $k_{\text{pol}}$  between the wild type and E288K; thus, the mutator ability opposite template A is not due to a large differential in incorporation rates. Instead, the E288K variant exhibits less discrimination at the level of  $K_{\text{d(dNTP)}}$  than wild-type pol  $\beta$  opposite template A. The discrimination at the level of  $K_{\text{d}}$  is reduced up to 7-fold in the E288K variant versus the wild-type pol  $\beta$ . Although wild-type pol  $\beta$  does not discriminate between dTTP and dCTP opposite template A, E288K actually prefers by a 7-fold margin to bind dCTP versus dTTP when A is the templating base. This tighter binding of incorrect nucleotides leads to a decrease in fidelity of 3–6-fold. The overall change in fidelity is also due in part to a 2-fold decrease in the ability of the E288K variant to bind to the correct nucleotide opposite template A.

**The Mutator Phenotype Is Specific for Template A.** To confirm that the mutagenic phenotype was specific for template A containing DNA, additional single-turnover experiments were conducted with one-base-gapped DNA substrates containing either C, G, or T in the gap as a templating base. There was no

**Table 3. Single-Turnover Kinetic Data for Wild-Type and E288K Pol  $\beta$  on One-Base-Gapped DNA Substrates Listed in Table 1**

template base <sup>a</sup>	dNTP	pol $\beta$ 288 <sup>b</sup>	$k_{\text{pol}}$ (s <sup>-1</sup> )	$K_{\text{d(dNTP)}}$ ( $\mu\text{M}$ )	D $k_{\text{pol}}$ <sup>c</sup>	D $K_{\text{d}}$ <sup>d</sup>	efficiency (M <sup>-1</sup> cm <sup>-1</sup> ) <sup>e</sup>	F <sup>f</sup>	x-fold <sup>g</sup>
A	dTTP	E	114 $\pm$ 10	66 $\pm$ 14			1700000		
		K	154 $\pm$ 18	123 $\pm$ 17			1300000		
	dATP	E	0.089 $\pm$ 0.003	440 $\pm$ 40	1300	6.7	200	8500	
		K	0.12 $\pm$ 0.01	220 $\pm$ 50	1300	1.8	550	2300	4
	dCTP	E	0.123 $\pm$ 0.005	64 $\pm$ 9	930	0.97	1900	900	
		K	0.161 $\pm$ 0.007	18 $\pm$ 4	960	0.15	8900	140	6
	dGTP	E	0.151 $\pm$ 0.007	190 $\pm$ 20	750	2.9	790	2200	
		K	0.209 $\pm$ 0.008	140 $\pm$ 20	740	1.2	1500	850	3
	dGTP	E	34 $\pm$ 2	17 $\pm$ 5			2000000		
		K	63 $\pm$ 11	11 $\pm$ 2			5700000		
C	dATP	E	0.169 $\pm$ 0.006	4.0 $\pm$ 0.8	200	0.23	42000	48	
		K	0.188 $\pm$ 0.005	2.0 $\pm$ 0.3	340	0.18	94000	61	0.8
	dCTP	E	0.17 $\pm$ 0.01	680 $\pm$ 170	200	40	250	8000	
		K	0.157 $\pm$ 0.009	190 $\pm$ 30	400	17	830	6900	1
	dTTP	E	0.30 $\pm$ 0.02	304 $\pm$ 50	110	18	990	2000	
		K	0.147 $\pm$ 0.004	16 $\pm$ 2	430	1.5	9200	620	3
	dCTP	E	27.4 $\pm$ 0.5	4.6 $\pm$ 0.5			6000000		
		K	34 $\pm$ 1	2.8 $\pm$ 0.5			12000000		
	dATP	E	0.0111 $\pm$ 0.0003	51 $\pm$ 6	2500	11	220	27000	
		K	0.041 $\pm$ 0.002	103 $\pm$ 17	830	37	400	31000	0.9
G	dGTP	E	0.0067 $\pm$ 0.0003	106 $\pm$ 19	4100	23	63	94000	
		K	0.0148 $\pm$ 0.0008	96 $\pm$ 21	2300	34	150	79000	1
	dTTP	E <sup>h</sup>	0.135 $\pm$ 0.007	42 $\pm$ 8	200	9.1	3200	1900	
		K	0.36 $\pm$ 0.02	132 $\pm$ 23	94	47	2700	4500	0.4
	dATP	E	51 $\pm$ 9	60 $\pm$ 10			850000		
		K	69 $\pm$ 2	34 $\pm$ 4			2000000		
	dCTP	E	0.25 $\pm$ 0.01	60 $\pm$ 10	200	1.0	4200	210	
		K	0.23 $\pm$ 0.01	15 $\pm$ 3	300	0.44	15000	130	2
	dGTP	E	0.38 $\pm$ 0.01	35 $\pm$ 4	130	0.58	11000	79	
		K	0.33 $\pm$ 0.02	7 $\pm$ 2	210	0.21	47000	44	2
T	dTTP	E	0.24 $\pm$ 0.02	310 $\pm$ 50	210	5.2	770	1100	
		K	0.183 $\pm$ 0.006	43 $\pm$ 6	380	1.3	4300	480	2

<sup>a</sup>See also Table 1: A, KDA; C, C2R; G, C2; T, KDAR. <sup>b</sup>E, wild type; K, E288K. <sup>c</sup>Discrimination of  $k_{\text{pol}} = k_{\text{pol(correct)}}/k_{\text{pol(incorrect)}}$ . <sup>d</sup>Discrimination of  $K_{\text{d(dNTP)}} = K_{\text{d(dNTP)(correct)}}/K_{\text{d(dNTP)(incorrect)}}$ . <sup>e</sup>Efficiency =  $k_{\text{pol}}/K_{\text{d(dNTP)}}$ . <sup>f</sup>Fidelity = [efficiency<sub>(correct)</sub> + efficiency<sub>(incorrect)</sub>]/efficiency<sub>(incorrect)</sub>. <sup>g</sup>x-fold change in fidelity = fidelity<sub>(WT)</sub>/fidelity<sub>(E288K)</sub>. <sup>h</sup>Incorporation of wild-type dTTP opposite template G (unpublished results of A. A. Nemec).

overall change in the fidelity of incorporation of a nucleotide opposite C, G, or T with E288K compared to the wild-type polymerase (Table 3).

**Substitution of Lysine for Glutamate at Residue 288 Moves Helix N.** Molecular modeling was conducted on the E288K variant ternary complexes with correct (dTTP) and incorrect (dCTP) nucleotides. The most notable structural alteration that occurs with the E288K variant is the movement of helix N. As shown in the crystal structures of pol  $\beta$ , helix N moves as a part of the large conformational change, helping to form the nucleotide binding pocket. Upon substitution of the glutamate with lysine in the ternary complex with the correct nucleotide, helix N is predicted to move 3.1 Å from its wild-type position (Figure 3a), as measured by the distance between the  $\alpha$ -carbon of residue 288 in the wild type and E288K. This movement would bring helix N closer to the DNA because of the change from a negatively charged side chain to a positively charged side chain. The lysine is drawn toward the electro-negative DNA phosphodiester backbone (His285-G5 downstream) by 6.4 Å [from 11 to 4.6 Å (Figure 3b)]. Interestingly, when E288K is modeled with an incorrect nucleotide (dCTP), helix N is predicted to move back 2.1 Å to a position that is more like that of the wild-type polymerase, without increasing the distance between helix N and the DNA (Figure 3b).

## DISCUSSION

Pol  $\beta$  is the major polymerase involved in BER, and in this capacity, it is responsible for the repair of many DNA lesions. Proper repair of lesions in the DNA is necessary for maintaining genomic integrity. A recent sequencing project identified the E288K variant of pol  $\beta$  in a colon tumor, and preliminary data suggested that this variant exhibited an enhanced ability to misincorporate nucleotides compared to the wild-type polymerase. The E288K variant has been determined through this work to in fact be a mutator mutant of pol  $\beta$ , possessing a decreased fidelity on DNA gaps with adenine template bases both in vivo and in vitro. This mutator ability is due to a decrease in the level of discrimination during nucleotide binding. The E288K variant prefers to bind to dCTP versus dTTP opposite template A with greater affinity. This reduced level of discrimination is likely due to movement of helix N to a more open conformation observed in the model of the variant, which could be impacting the nucleotide binding pocket.

**E288K Is a Low-Fidelity Variant of Pol  $\beta$ .** The E288K variant was expressed in cells containing the  $\lambda$  phage genome, and a forward mutation assay was conducted looking at mutants in the  $\lambda cII$  gene. There was no increase in the overall mutation frequency in cells expressing E288K compared to the

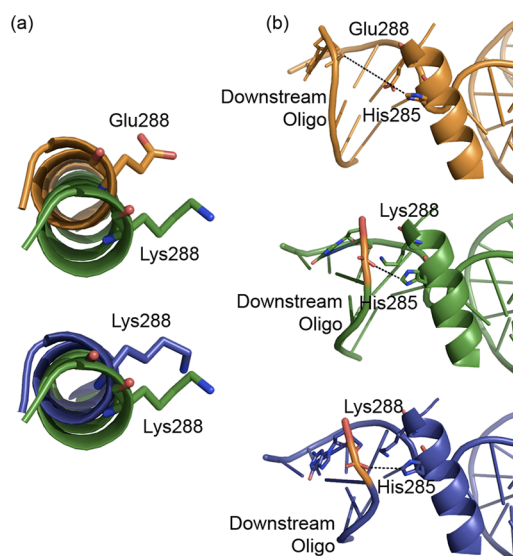


**Figure 3.** Molecular modeling of wild-type and E288K pol  $\beta$ . The wild-type pol  $\beta$  structure (Protein Data Bank entry 2FMS) is colored orange, E288K with the correct nucleotide (dTTP) green, and E288K with the incorrect nucleotide (dCTP) blue. (a) Helix N (Asp276–Gly290) moves 3.1 Å away from its wild-type position when residue 288 is lysine (top) and moves 2.1 Å back toward the wild-type position in the presence of an incorrect nucleotide (bottom). (b) The downstream oligo of the DNA substrate and His285 on helix N move closer together upon substitution of residue 288 with lysine (11.0, 4.6, and 4.4 Å, respectively).

same cells not expressing E288K. Examining the types of mutations revealed an increase in mutation frequency at AT base pairs (Table 2). Under single-turnover conditions on a one-base-gapped substrate, E288K exhibits a 3–6-fold decreased fidelity opposite template A (Table 3). In the case of template A, the loss of fidelity is due to defects in normal nucleotide binding in a two-pronged manner. First, E288K has a 2-fold decreased level of binding to the correct nucleotide (dTTP), and second, the variant has an up to 4-fold increased level of binding to the incorrect nucleotide, compared to that of the wild-type polymerase. All this is with very little change in the maximal polymerization rate ( $k_{\text{pol}}$ ) for the mutant, indicating that the decreased fidelity is due to changes in nucleotide binding. Misincorporation of dCTP opposite A yields a 6-fold loss of fidelity with E288K. Additionally, the wild type has no discrimination at the level of nucleotide binding for dCTP opposite template A, which means that wild-type pol  $\beta$  cannot distinguish between dCTP and dTTP during binding.

In the case of one-base-gapped DNAs with template bases other than A, E288K is not a mutator. The variant has a  $\leq 2$ -fold decrease in fidelity compared to that of the wild type, opposite templates C, G, and T. There is one interesting exception, and that is the case of dTTP inserted opposite template C. In this case, there is a slight (3-fold) decrease in fidelity with the E288K variant. This decrease is due to the large change in  $K_{\text{d(dNTP)}}$  for this incorporation, which is 19-fold lower compared to that of the wild type. This trend is observed with all incorporation events involving pyrimidine nucleotides opposite pyrimidine templates. In each case, E288K has a decreased discrimination at the level of binding to the dNTP substrate compared to that of the wild type (4–19-fold). This is possibly due to the movement of helix N toward a more open conformation.

**Helix N May Move to a More Open Position in the E288K Variant.** Molecular modeling suggests that when the glutamate at position 288 is replaced with lysine, helix N shifts  $\sim 3.1$  Å (Figure 3a). This movement is toward the downstream oligo of the DNA substrate (Figure 3b), which may indicate that the E288K variant exists in a more open conformation than the wild-type polymerase. This could be an indication that the binding pocket in E288K is malformed in some way, as helix N moves during the large subdomain movement conformational change to help produce the nucleotide binding pocket.<sup>11</sup> The kinetic data show that there are alterations in nucleotide binding but not in polymerization rate for the E288K variant, which suggests that the binding pocket may not be in its ideal conformation while the active site is functioning properly like the wild-type polymerase. In fact, other mutants located along helix N have shown similar changes in nucleotide binding with little effect on  $k_{\text{pol}}$ .<sup>10,16</sup> The fact that this defect in E288K is specific for a single templating base and to some extent pyrimidines opposite pyrimidines would indicate that this is a subtle change in the binding pocket, and the model suggests that helix N is moving only 3.1 Å at residue 288, which is at the distal end of the helix relative to the binding pocket. When dCTP is modeled in opposite template A, the model indicates that helix N could move 2.1 Å back toward the wild-type position relative to the Lys288 model with dTTP. This may lead to a more wild-type-like binding pocket and could result in tighter binding of the incorrect dCTP. The fact that the model does not predict any change in the distance between helix N and the DNA between the E288K models with dTTP and dCTP could be an indication that the DNA in the active site is shifted in both cases; thus, E288K may exhibit a preference for binding dCTP over dTTP opposite template A. This predicted movement of helix N may be causing a disruption or an enlargement of the binding pocket, which would lead to altered binding of nucleotides by the E288K variant relative to that of the wild type. Although these molecular dynamics simulations can give an idea of what the structure of the E288K variant could resemble, another approach would include computational analysis of the free energies of the transition state.<sup>17</sup>

An increased affinity for incorrect nucleotides opposite template A was demonstrated kinetically to be responsible for the reduced fidelity of E288K. The decreased fidelity has also been observed in cell culture, where in a forward mutation assay there was also an increase in the frequency of mutations at adenine bases. This mutator phenotype of the E288K variant may lead to an increased level of mutagenesis and, as a result, genomic instability, which could ultimately lead to a malignant tumor phenotype.

## ■ ASSOCIATED CONTENT

### 📄 Supporting Information

PCR and sequencing primer sequences, DNA oligos for one-base-gapped DNA substrate construction, circular dichroism and thermal stability data, C127 $\lambda$ b expression Western blot, and a  $\lambda$ cII forward mutation spectrum. This material is available free of charge via the Internet at <http://pubs.acs.org>.

## ■ AUTHOR INFORMATION

### Corresponding Author

\*Departments of Therapeutic Radiology and Genetics, Yale University School of Medicine, New Haven, CT 06520. E-mail: joann.sweasy@yale.edu. Telephone: (203) 737-2626. Fax: (203) 785-6309.

# Funding

Supported by National Institute of Environmental Health Sciences Grant RO1 ES019179.

# Notes

The authors declare no competing financial interest.

# ■ ACKNOWLEDGMENTS

We thank A. Keh for her help and expertise in the *λcII* forward mutation assay and J. Yamtich for helpful advice and discussions regarding this work.

# ■ ABBREVIATIONS

BER, base excision repair; dRP, deoxyribose phosphate; pol  $\beta$ , DNA polymerase  $\beta$ .

# ■ REFERENCES

- (1) Lindahl, T. (1993) Instability and decay of the primary structure of DNA. *Nature* 362, 709–715.
- (2) Prasad, R., Beard, W. A., Strauss, P. R., and Wilson, S. H. (1998) Human DNA polymerase  $\beta$  deoxyribose phosphate lyase. Substrate specificity and catalytic mechanism. *J. Biol. Chem.* 273, 15263–15270.
- (3) Starcevic, D., Dalal, S., and Sweasy, J. B. (2004) Is there a link between DNA polymerase  $\beta$  and cancer? *Cell Cycle* 3, 998–1001.
- (4) Venkatesan, R. N., Bielas, J. H., and Loeb, L. A. (2006) Generation of Mutator Mutants during Carcinogenesis. *DNA Repair* 5, 294–302.
- (5) Sweasy, J. B., Lang, T., Starcevic, D., Sun, K. W., Lai, C. C., Dimaio, D., and Dalal, S. (2005) Expression of DNA polymerase  $\beta$  cancer-associated variants in mouse cells results in cellular transformation. *Proc. Natl. Acad. Sci. U.S.A.* 102, 14350–14355.
- (6) Lang, T., Dalal, S., Chikova, A., DiMaio, D., and Sweasy, J. B. (2007) The E295K DNA polymerase  $\beta$  gastric cancer-associated variant interferes with base excision repair and induces cellular transformation. *Mol. Cell. Biol.* 27, 5587–5596.
- (7) Dalal, S., Chikova, A., Jaeger, J., and Sweasy, J. B. (2008) The Leu22Pro tumor-associated variant of DNA polymerase  $\beta$  is dRP lyase deficient. *Nucleic Acids Res.* 36, 411–422.
- (8) Donigan, K. A., Hile, S. E., Eckert, K. A., and Sweasy, J. B. (2012) The human gastric cancer-associated DNA polymerase  $\beta$  variant D160N is a mutator that induces cellular transformation. *DNA Repair* 11, 381–390.
- (9) Dalal, S., Hile, S., Eckert, K. A., Sun, K. W., Starcevic, D., and Sweasy, J. B. (2005) Prostate-cancer-associated I260M variant of DNA polymerase  $\beta$  is a sequence-specific mutator. *Biochemistry* 44, 15664–15673.
- (10) Murphy, D. L., Kosa, J., Jaeger, J., and Sweasy, J. B. (2008) The Asp285 variant of DNA polymerase  $\beta$  extends mispaired primer termini via increased nucleotide binding. *Biochemistry* 47, 8048–8057.
- (11) Murphy, D. L., Jaeger, J., and Sweasy, J. B. (2011) A triad interaction in the fingers subdomain of DNA polymerase  $\beta$  controls polymerase activity. *J. Am. Chem. Soc.* 133, 6279–6287.
- (12) Johnson, K. A. (1993) Conformational coupling in DNA polymerase fidelity. *Annu. Rev. Biochem.* 62, 685–713.
- (13) Glazer, P. M., Sarkar, S. N., and Summers, W. C. (1986) Detection and analysis of UV-induced mutations in mammalian cell DNA using a  $\lambda$  phage shuttle vector. *Proc. Natl. Acad. Sci. U.S.A.* 83, 1041–1044.
- (14) Gunther, E. J., Murray, N. E., and Glazer, P. M. (1993) High efficiency, restriction-deficient in vitro packaging extracts for bacteriophage  $\lambda$  DNA using a new *E. coli* lysogen. *Nucleic Acids Res.* 21, 3903–3904.
- (15) Yamtich, J., Starcevic, D., Lauper, J., Smith, E., Shi, I., Rangarajan, S., Jaeger, J., and Sweasy, J. B. (2010) Hinge residue I174 is critical for proper dNTP selection by DNA polymerase  $\beta$ . *Biochemistry* 49, 2326–2334.
- (16) Shah, A. M., Conn, D. A., Li, S. X., Capaldi, A., Jager, J., and Sweasy, J. B. (2001) A DNA polymerase  $\beta$  mutator mutant with

reduced nucleotide discrimination and increased protein stability. *Biochemistry* 40, 11372–11381.

(17) Ram Prasad, B., and Warshel, A. (2011) Prechemistry versus preorganization in DNA replication fidelity. *Proteins* 79, 2900–2919.